Received: 15 October 2019 | Revised: 8 January 2020 | Accepted: 8 January 2020

DOI: 10.1002/jcc.26153

FULL PAPER

Journal of COMPUTATIONAL CHEMISTRY WILEY

Improving the predictive quality of time-dependent density functional theory calculations of the X-ray emission spectroscopy of organic molecules

Adam A. E. Fouda | Nicholas A. Besley

School of Chemistry, University of Nottingham, Nottingham

Correspondence
Nicholas A. Besley, School of Chemistry, University of Nottingham, University Park, Nottingham NG7 2RD, UK
Email: nick.besley@nottingham.ac.uk

Funding information
Leverhulme Trust, Grant/Award Number: RPG-2016-103

Abstract

The simulation of X-ray emission spectra of organic molecules using time-dependent density functional theory (TDDFT) is explored. TDDFT calculations using standard hybrid exchange-correlation functionals in conjunction with large basis sets can predict accurate X-ray emission spectra provided an energy shift is applied to align the spectra with experiment. The relaxation of the orbitals in the intermediate state is an important factor, and neglect of this relaxation leads to considerably poorer predicted spectra. A short-range corrected functional is found to give emission energies that required a relatively small energy shift to align with experiment. However, increasing the amount of Hartree–Fock exchange in this functional to remove the need for any energy shift led to a deterioration in the quality of the calculated spectral profile. To predict accurate spectra without reference to experimental measurements, we use the CAM-B3LYP functional with the energy scale determined with reference to a Δself-consistent field calculation for the highest energy emission transition.

KEYWORDS
organic molecules, TDDFT, XES, X-ray emission spectroscopy

1 | INTRODUCTION

The availability of improved X-ray light sources has led to an increased interest in spectroscopic techniques in the X-ray region. One attraction of these techniques is that they provide an element specific, local probe of geometric and electronic structure, and they have been applied to study a wide variety of applications, ranging from biological systems to materials.[1–3] X-ray emission spectroscopy (XES) measures the X-ray emission following ionization of a core electron and can be performed under non-resonant or resonant conditions. XES probes the occupied molecular orbitals and is complementary to X-ray absorption spectroscopy (XAS) which is sensitive to the unoccupied orbitals. XES is a widely used technique that has been used to probe the structure of liquids[4] and the absorption of molecules on surfaces.[1]

Accurate simulation of X-ray emission spectra can play a vital role in the assignment of the spectral bands and enable the full interpretation of the experimental data. A number of different theoretical approaches have been developed and applied to the study of XES. The most formally straightforward approach to determine the energy and associated oscillator strengths for the various valence to core transitions required to simulate an X-ray emission spectrum is to approximate the transitions energies using the energy difference between the orbital energies

$$\Delta E = \epsilon_v - \epsilon_c \quad (1)$$

and estimate the oscillator strengths from

$$f \propto |\langle \phi_c | \hat{\mu} | \phi_v \rangle|^2, \quad (2)$$

where ϕ_c is a core orbital and ϕ_v is a valence orbital. This approach has been used successfully in many studies, for example, the study of valence-to-core XES of transition metal complexes.[5,6] One of the important advantages of this approach is that it allows the spectra to be determined directly from the wavefunction[7–10] or Kohn–Sham density functional theory (DFT)[5] calculations.

Following ionization of a core electron, the effective nuclear charge of the relevant nuclei increases by one, and as a consequence the molecular orbitals will adapt to the new environment. This relaxation of the electronic structure in the presence of the core hole is described explicitly in Δself-consistent field (SCF) approaches. In this approach, separate SCF calculations are performed for each core-ionized final state. The transition energies are then given by the difference in the electronic-state energies and the transition dipole moments evaluated between the wavefunctions for the initial and final states. This approach has been shown to provide accurate core-ionization energies[11–15]; however, it is difficult to apply to large systems owing to the number of individual SCF calculations required, and the challenge of performing SCF calculations for arbitrary electronic states. This has led to the development of methods that incorporate the electronic relaxation while avoiding the practical limitations of ΔSCF. For example, in the $Z + 1$ approximation, an increased nuclear charge is used for the absorbing atom[16] or the transition potential approach where a half filled core orbital is used providing a balance between final and initial states.[17]

More recently, an alternative approach to computing X-ray emission spectra using conventional response theory methods, such as time-dependent DFT (TDDFT), was introduced. In this scheme, the determinant for the state with a core hole is used as a reference and the transitions of interest are found as those with negative eigenvalues.[18] In this approach, the relaxation of the orbitals in the presence of the core hole is captured by the core-ionized reference determinant. This has been applied within the context of equation-of-motion coupled cluster theory,[19] TDDFT[20] and the algebraic construction methods.[21] An advantage of this approach compared with ΔSCF is that the complete spectrum can be determined in a single calculation. The XES of transition metal systems have been studied using TDDFT,[22–24] and it has been shown that the experimental spectra are reproduced well although an energy shift needs to be applied to the calculated spectra to align with experiment. This compromises the predictive power of TDDFT and is a consequence of deficiencies in the exchange-correlation functional associated with the electron self-interaction error.[20] There has been less focus on the calculation of the XES of organic molecules, although studies of water[25] and a small selection of organic molecules[20] have been reported. In the latter study, an attempt was made to parameterize a hybrid exchange-correlation functional to describe the X-ray emission energies more accurately. However, although the systematic overestimation of the excitation energies was reduced by increasing the fraction of Hartree–Fock exchange in the functional, the calculated spectral profiles were adversely affected.

The choice of Gaussian basis set has emerged as another important factor in the accuracy of these calculations.[26] The higher effective nuclear charge results in a contraction of the electron density in the core-ionized state. Small or moderately sized basis sets can provide a poor description of the core-ionized state because they do not have the flexibility to describe the more compact electron density. This is particularly a problem for the study of XES at the *K*-edge of heavier nuclei. One solution is to simply use very large basis sets such as large Dunning basis sets with core-correlation functionals, such as cc-pCVTZ and cc-pCVQZ, which have been shown to be effective.[23] However, this can severely restrict the size of system that can be studied. Alternative basis sets that achieve a balanced description of the ground and core-ionized states have been proposed including using exponents for the basis functions midway between the element and the element with a nuclear charge of one higher[27] and explicitly including basis functions for the $Z + 1$ element in the basis set.[28]

In this study, we investigate the accuracy of TDDFT calculations for a range of organic molecules and explore the dependence of the computed spectra on factors such as basis set, exchange-correlation functional and the relaxation of the intermediate state. It is shown that accurate spectra can be computed from first principles following the application of an energy shift derived from DFT calculations for the highest energy transition and that the CAM-B3LYP functional provides a reliable description of the spectral band profile, providing a new protocol for reliably predicting XES spectra.

2 | METHODOLOGY

X-ray emission spectra were computed with TDDFT within the Tamm–Dancoff approximation[29] using a protocol described previously.[20] Following a Kohn–Sham DFT calculation for the ground state, a further DFT calculation is performed for the core-ionized state with the maximum overlap method[30] used to maintain the core-hole during the SCF procedure and in a subsequent TDDFT calculation using the core-ionized state as a reference the emission energies appear as negative eigenvalues. Calculations were performed for the following molecules: methanol (carbon *K*-edge), ammonia (nitrogen *N*-edge), acetone and dimethyl sulfoxide (DMSO) (oxygen *K*-edge), fluorobenzene (fluorine *K*-edge), H_2S (sulfur *K*-edge), CH_3Cl, and CF_3Cl (chlorine *K*-edge) and compared with experimental data adapted from ref.[31–36] The structures of the molecules were optimized at the B3LYP/6-311G** level of theory. Relativistic effects can also be significant, and these effects are accounted for by applying an energy shift to the computed transition energies. The magnitude of this shift is determined from the difference in the 1s orbital energy between relativistic and nonrelativistic HF/cc-pCVQZ-DK[37] with the relativistic effects modeled using the Douglas–Kroll–Hess Hamiltonian. This gives values of +0.13, +0.25, +0.44, +0.47, +0.74, +10.01, +13.08, and +13.08 eV for methanol, ammonia, acetone, DMSO, fluorobenzene, H_2S, CH_3Cl, and CF_3Cl, respectively. All calculations were

performed with the Q-CHEM software package.[38] Computational spectra were generated by convoluting the computed energies and oscillator strengths with Gaussian functions with full width at half maximum of 0.25 eV.

3 | RESULTS AND DISCUSSION

We begin our analysis by demonstrating the accuracy that is obtained using TDDFT with a standard hybrid functional to simulate X-ray emission spectra before proceeding to explore how various approximations affect the quality of the computed spectra and the dependence on the exchange-correlation functional. The accuracy that can be obtained from TDDFT calculations of XES is represented in Figure 1, which shows a comparison between the computed and experimental spectra for a range of molecules at the *K*-edge involving a variety of nuclei. The spectra are computed with the cc-pCVQZ basis set and the B3LYP exchange-correlation functional, and an energy shift has been applied to each spectra so that the most intense peak aligns with the experimental data. The magnitude of these shifts is given in the figure caption, and these shifts are in addition to the energy correction due to relativistic effects. The cc-pCVQZ basis set is large and has been shown to give emission energies that are converged with respect to the basis set.[26] The computed spectra reproduce the experimental spectra remarkably well. For all of the molecules, the computed spectra predict the peak heights and their relative energy spacing with a high degree of accuracy. In some spectra, most notably ammonia and H_2S, the experiment has bands at higher emission energy which can be associated with elastic scattering and multielectron transitions.[33,34] Multielectron transitions of this type will not be described by the TDDFT methodology used here. In some cases the relative intensities of the bands are not predicted in line with experiment, for example, for ammonia and acetone. However, a uniform broadening has been applied and a single structure considered, and so the effects of nuclear dynamics are not accounted for. Consideration of nuclear dynamics can affect the relative

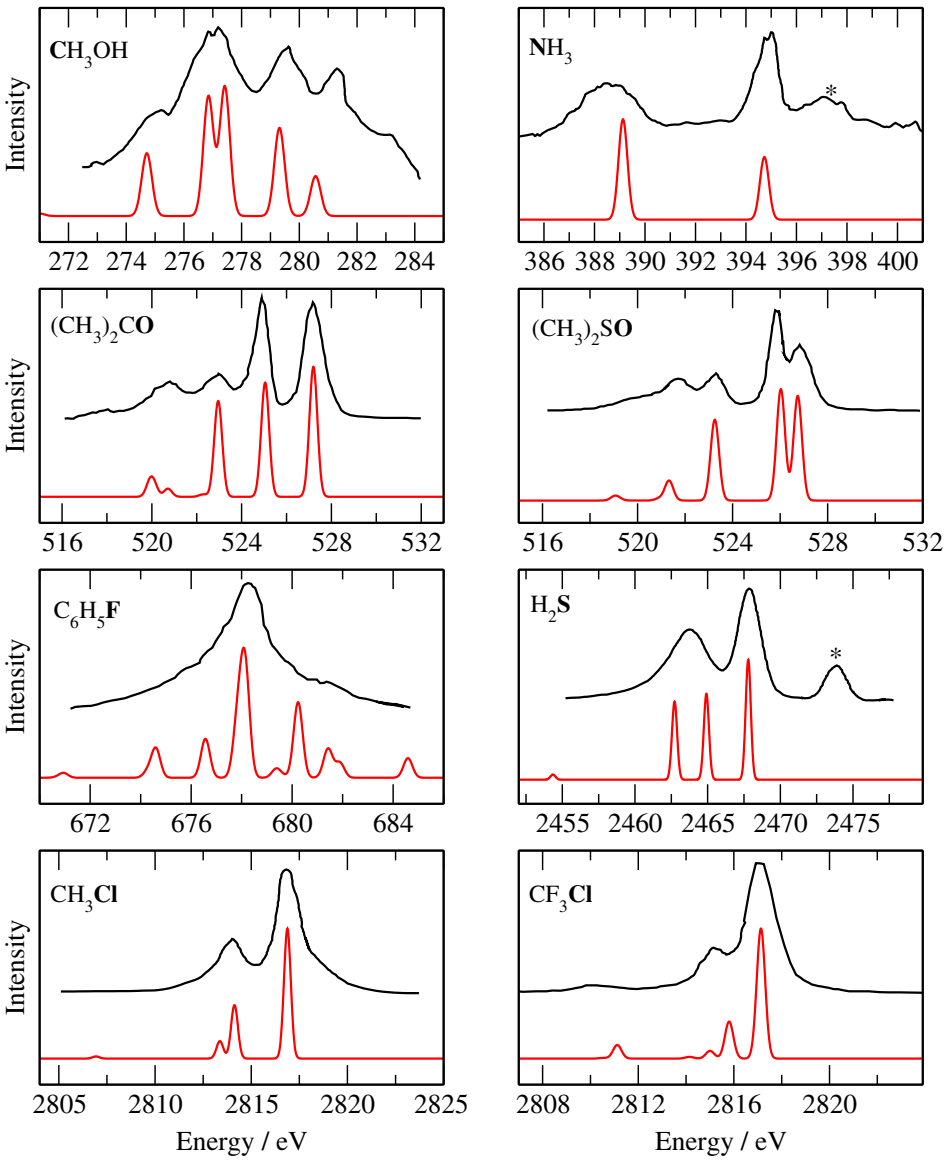

FIGURE 1 Calculated B3LYP/cc-pCVQZ and experimental X-ray emission spectra for **C**H_3OH, **N**H_3, $(CH_3)_2$**C**O, $(CH_3)_2$**S**O, C_6H_5**F**, H_2**S**, CH_3**Cl** and CF_3**Cl**, with bold font denoting the atom that has been core-ionized. Black line: experiment and red line: calculation. Asterisk mark indicates a multielectron feature. The following energy shifts have been applied to the calculated spectra to align them with experiment CH_3OH: −6.3 eV, NH_3: −6.9 eV, $(CH_3)_2CO$: −8.8 eV, $(CH_3)_2SO$: −8.6 eV, C_6H_5F: −7.9 eV, H_2S: −33.7 eV, CH_3Cl: −32.9 eV, and CF_3Cl: −32.9 eV [Color figure can be viewed at wileyonlinelibrary.com]

intensities of the bands, and as shown in Appendix S1 for ammonia, averaging over structures from an ab initio molecular dynamics simulation of the core-ionized state does result in the higher energy band becoming relatively more intense than the lower energy band.

As noted above and in the figure caption, an energy shift is required to align the computed spectra with experiment. The calculations systematically overestimate the emission energies. This is in contrast to TDDFT calculations of X-ray absorption spectra where the transition energies are underestimated. However, both of these errors are a manifestation of the self-interaction error.[18,39] In the context of X-ray absorption calculations, the self-interaction error leads to the energy of the occupied core orbitals being too high resulting in an underestimation of the core → virtual orbital energy differences. We note that electron correlation is also important and neglect of electron correlation, for example in a time-dependent Hartree–Fock calculation, leads to an overestimation of the core-excitation energies. For X-ray emission calculations, it leads to the energy of the unoccupied core orbital in the reference core-ionized state being too low leading to an overestimation of the valence → virtual-core orbital energy differences. This artifact is less prevalent in ΔSCF calculations where the orbitals are optimized for each state and the virtual orbitals do not play a direct role. The magnitude of the shift applied increases as the nuclear charge of the ionized nuclei increases. For the examples shown here, the size of the shift applied varies from −6.3 eV for the methanol carbon and −32.9 eV for the chorine in CF_3Cl.

Analogous spectra computed with TDDFT where there is no electronic relaxation in the intermediate state are shown in Figure 2. These spectra are computed using the same approach except the reference determinant is comprised of the orbitals for the neutral ground state with a vacancy introduced to the appropriate core orbital. The neglect of relaxation leads to a large change in the calculated spectra and the resulting spectra show a considerably worse agreement with experiment, and for some of the molecules the calculated spectra show little resemblance to experiment. This is consistent with previous work on transition metal complexes that also found TDDFT spectra derived from the unrelaxed orbitals to have a worse agreement

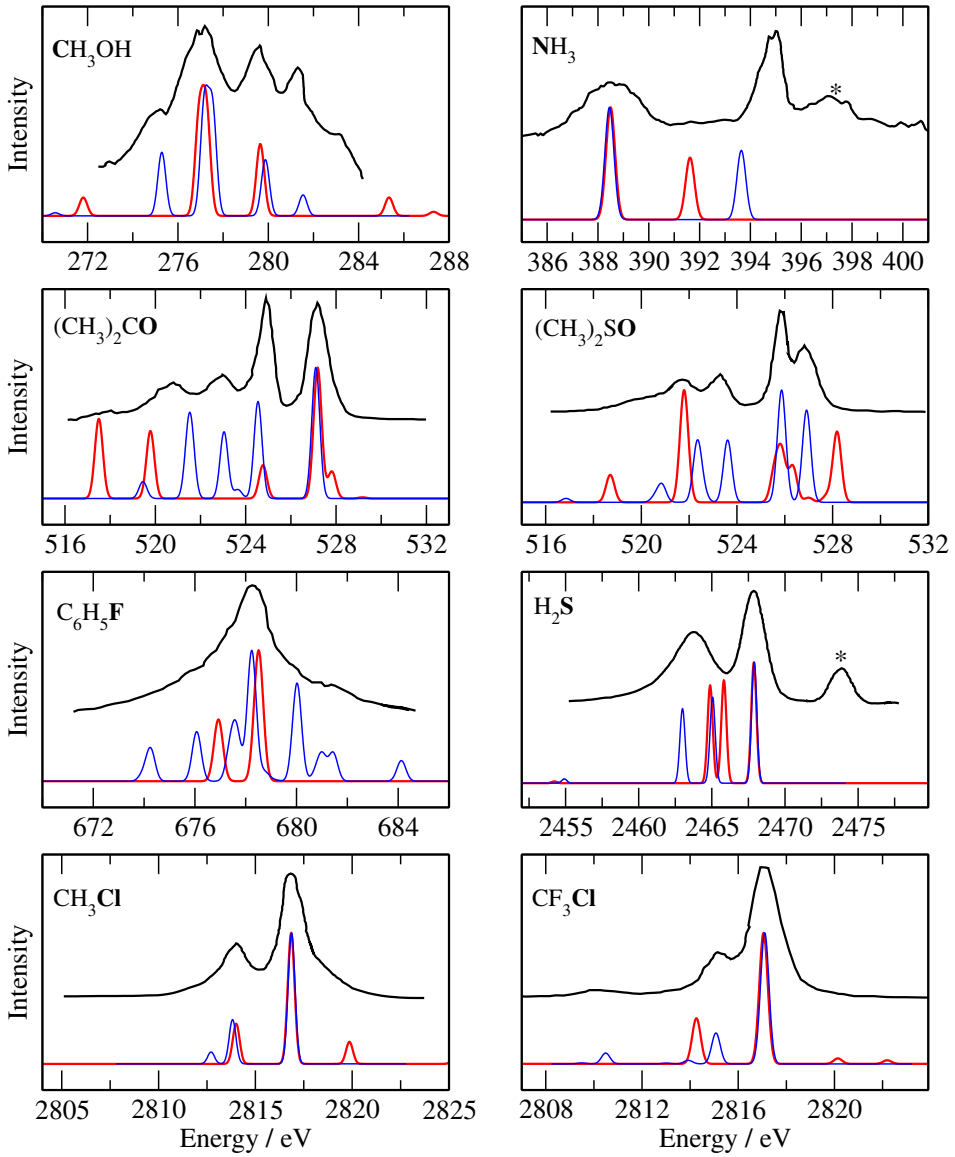

FIGURE 2 Calculated TDDFT B3LYP/cc-pCVQZ with no orbital relaxation (red line), Kohn–Sham DFT B3LYP/cc-pCVQZ (blue line) and experimental X-ray emission spectra (black line) for CH_3OH, NH_3, $(CH_3)_2CO$, $(CH_3)_2SO$, C_6H_5F, H_2S, CH_3Cl, and CF_3Cl, with bold font denoting the atom that has been core-ionized. Asterisk mark indicates a multielectron feature. The following energy shifts have been applied to the calculated spectra to align them with experiment CH_3OH: −25.2 eV, NH_3: −30.9 eV, $(CH_3)_2CO$: −46.0 eV, $(CH_3)_2SO$: −46.6 eV, C_6H_5F: −34.4 eV, H_2S: −86.7 eV, CH_3Cl: −91.1 eV and CF_3Cl: −91.6 eV for TDDFT and CH_3OH: +11.1 eV, NH_3: +11.9 eV, $(CH_3)_2CO$: +13.5 eV, $(CH_3)_2SO$: +13.6 eV, C_6H_5F: +18.5 eV, H_2S: +47.1 eV, CH_3Cl: +49.7 eV and CF_3Cl: +50.2 eV for Kohn–Sham DFT. TDDFT, time-dependent density functional theory [Color figure can be viewed at wileyonlinelibrary.com]

with experiment.[22] Also shown in Figure 2 are spectra computed based upon the Kohn–Sham ground-state orbitals using Equations (1) and (2). This approach to computing the spectra also does not incorporate any orbital relaxation in the core-ionized state but in contrast to the TDDFT calculations provides an accurate representation of the experimental spectra. This suggests that there is some cancellation of errors between approximating the transition as the orbital energy difference and the relaxation in the intermediate state. The two conditions studied here, namely, full and no relaxation, represent the two extreme situations. Depending on the relative timescales of the electronic relaxation and the core-hole lifetime, it is possible to conceive of situations where only partial relaxation may occur.

We investigate next the role of the basis set on the calculated spectra. Figure 3 shows the calculated spectra for a range of basis sets of varying quality for DMSO and CF_3Cl, and the energy differences with respect to the cc-pCVQZ basis set for all of the molecules are given in Table 1. For these spectra, no energy shift has been applied. The results show that varying the quality of the basis set has a relatively small effect on the spectral profile but does have a significant effect on the calculated emission energies, particularly at the Cl

TABLE 1 Energy difference relative to the cc-pCVQZ basis set for the most intense band for the basis sets studied

Molecule	cc-VTZ	IGLO-II	6-31G*	(Z + 1)6-31G*
CH_3OH	+0.56	+0.19	+2.98	+0.55
NH_3	+0.78	+0.25	+4.43	+0.73
$(CH_3)_2$**C**O	+1.03	+0.26	+5.17	+0.75
$(CH_3)_2$**S**O	+1.15	+0.26	+5.22	+0.73
C_6H_5**F**	+1.24	+0.28	+5.60	+0.84
H_2**S**	+20.37	+0.59	+32.47	+0.45
CH_3**Cl**	+21.47	+0.51	+32.52	+0.30
CF_3**Cl**	+21.44	+0.51	+32.33	+0.30

Bold font denotes the atom that is core-ionized.

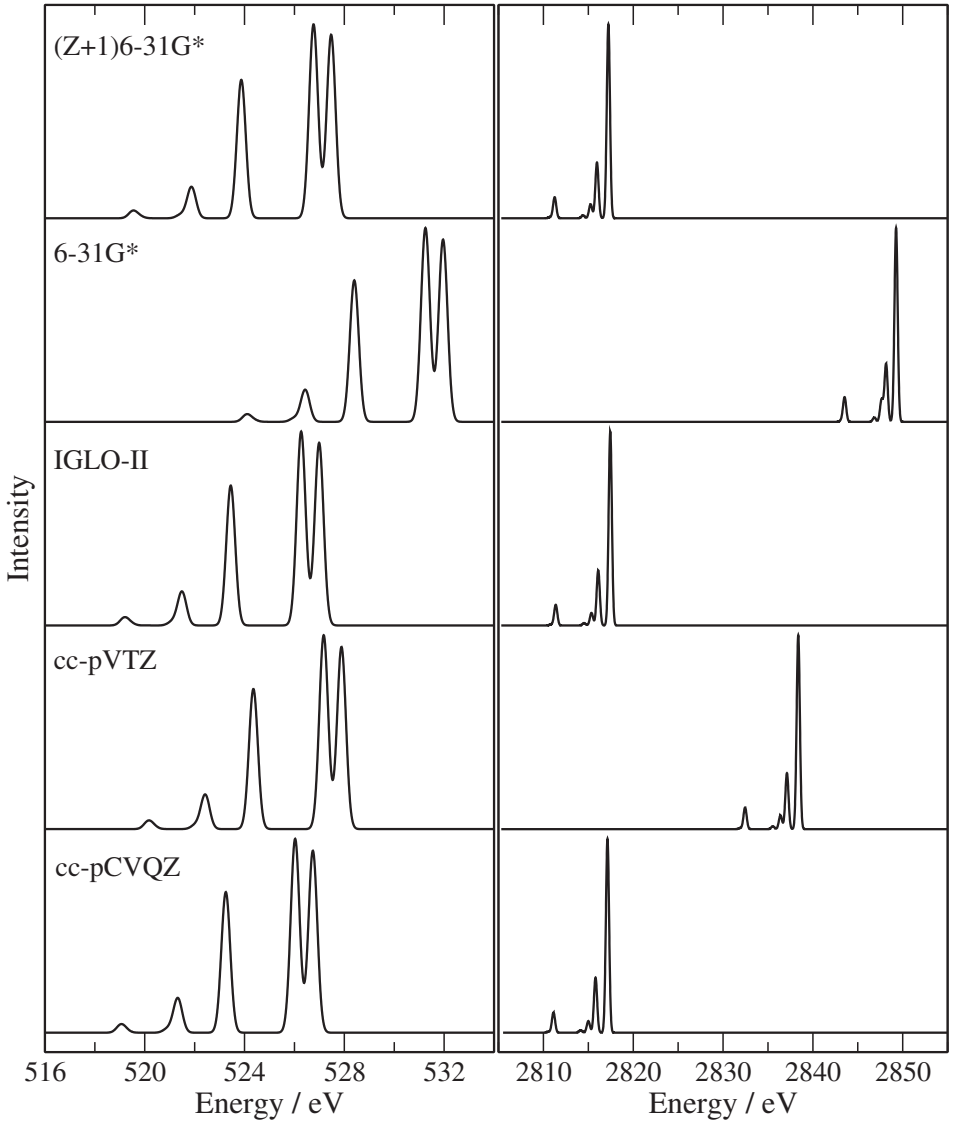

FIGURE 3 Variation of the calculated spectra with basis set for oxygen *K*-edge of DMSO (left) and chlorine *K*-edge of CF_3Cl (right). Spectra computed with the B3LYP exchange-correlation functional. DMSO, dimethyl sulfoxide [Color figure can be viewed at wileyonlinelibrary.com]

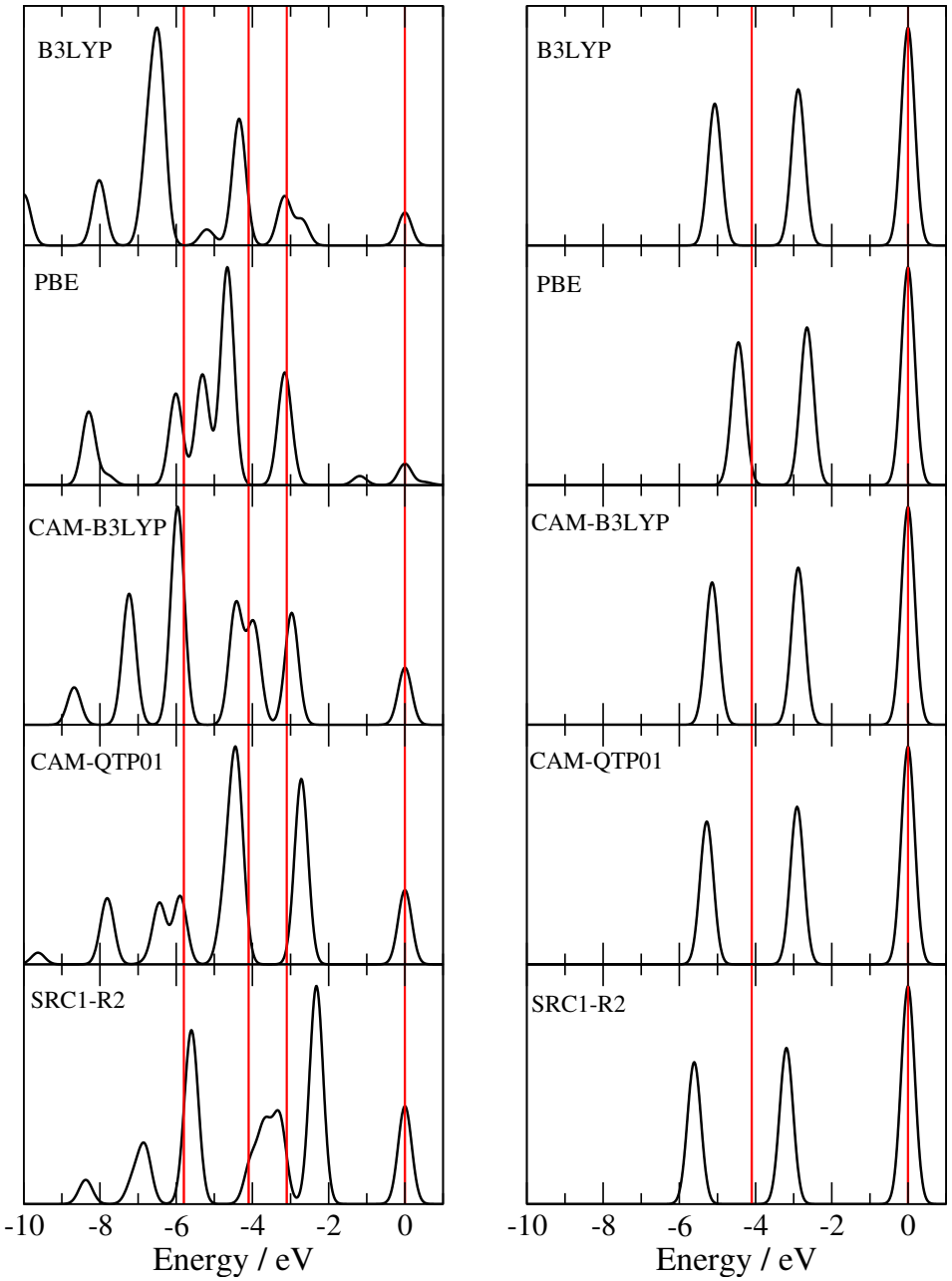

FIGURE 4 Variation of computed X-ray emission spectra with exchange-correlation functional for C_6H_5**F** (left) and H_2**S** (right) with the cc-pCVQZ basis set. The spectra are plotted relative to the energy of the highest energy band which is set to zero, and the vertical red lines indicate the position of the bands in the experimental spectra [Color figure can be viewed at wileyonlinelibrary.com]

K-edge. This is consistent with the findings of previous studies.[26] It is of interest to have small basis sets that are able to replicate the results of the much larger basis sets at a vastly reduced computational cost. In this regard, the IGLO-II basis set performs well, and this has been recognized previously in the literature.[40,41] The (*Z* + 1)6-31G* basis set also performs well. This is a nonstandard approach that was introduced recently,[28] and involves supplementing the 6-31G* basis set with basis functions for the element with nuclear charge one greater for the element being ionized. While the individual gauge for localised orbitals (IGLO) basis sets are only available for a subset of the elements, this (*Z* + 1) protocol can be applied to generate basis sets for all elements.

Figures 4 and 5 show computed spectra for fluorobenzene, H_2S, CH_3Cl, and CF_3Cl with the exchange-correlation functionals: B3LYP, PBE,[42] CAM-B3LYP,[43] CAM-QTP(01)[44] and SRC1-R2[45] evaluated using the cc-pCVQZ basis set. In these figures, the spectra are plotted relative to the energy of the highest energy band to allow an easier comparison of the spectral profiles. Analogous figures for methanol, ammonia, acetone, and DMSO are provided in Appendix S1. The functionals were chosen from a survey of a wide range of functionals as providing X-ray emission energies close to the experimental values. SRC1-R2 is a short-range corrected functional that was parameterized for XAS, while CAM-B3LYP and CAM-QTP(01) are range-separated functional with 100% HF exchange in the long range. The CAM-QTP

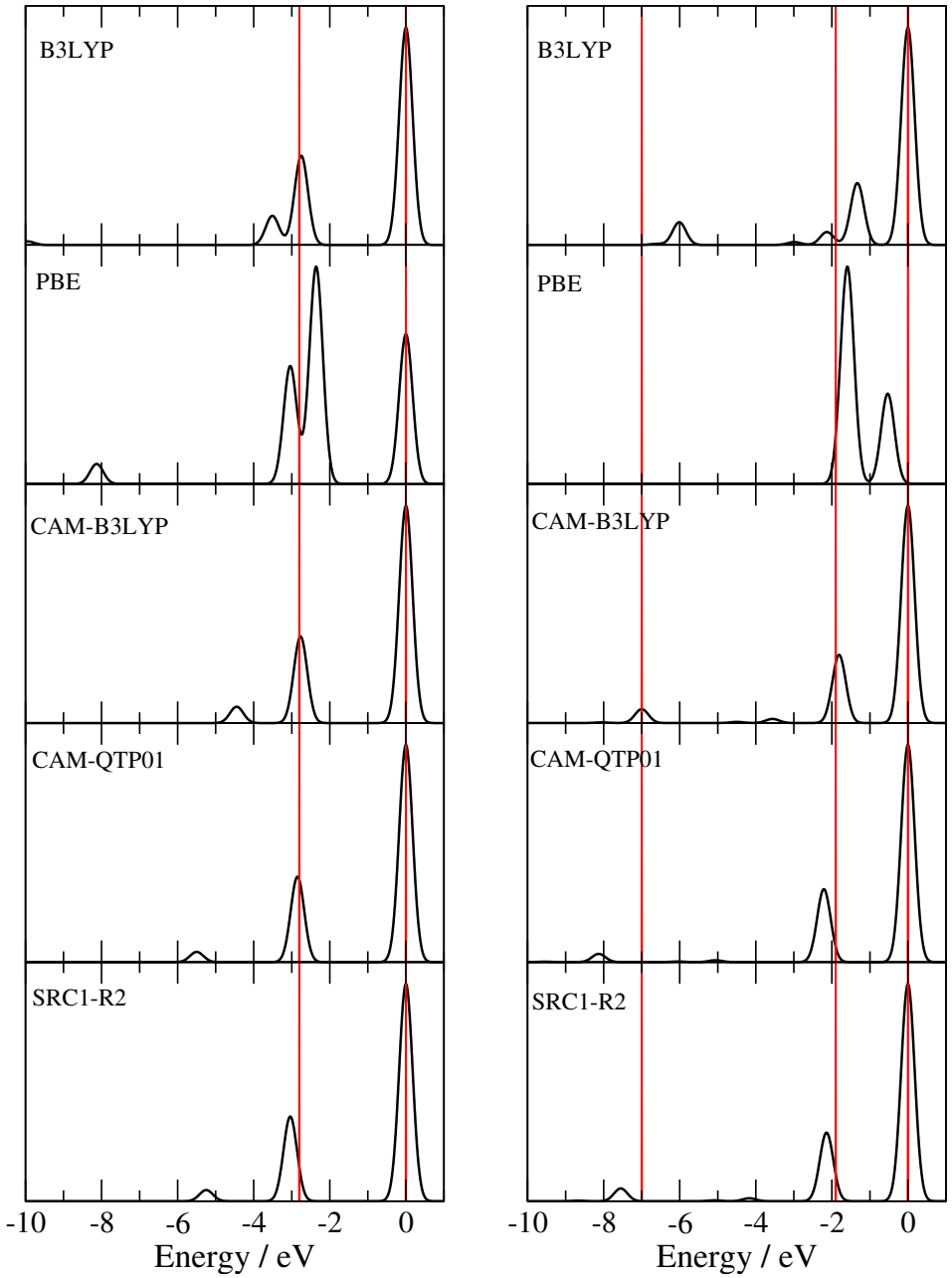

FIGURE 5 Variation of computed X-ray emission spectra with exchange-correlation functional for CH_3**Cl** (left) and CF_3**Cl** (right) with the cc-pCVQZ basis set. The spectra are plotted relative to the energy of the highest energy band which is set to zero, and the vertical red lines indicate the position of the bands in the experimental spectra [Color figure can be viewed at wileyonlinelibrary.com]

(01) functional is parameterized so that the Kohn–Sham eigenvalues are approximately equal to the vertical ionization energies.

The spectral profiles predicted by the different functionals are qualitatively similar. The exception to this is PBE which gives distinctly poorer spectra for acetone, DMSO, and CF_3Cl. On balance, the CAM-B3LYP functional gives a good description of the relative energies of the bands observed in experiment, showing some improvement over B3LYP. We now focus on which functional gives predicted excitation energies that are in agreement with experiment so that no energy shift is required to align the calculated spectra with experiment. Table 2 shows the energy difference between the calculated spectra and experiment for the most intense band. All of the functionals considered overestimate the transition energies but a common pattern emerges across the molecules. The generalised gradient approximation (GGA) functional PBE shows the greatest overestimation, while the values for B3LYP and CAM-B3LYP are quite similar. The CAM-QTP(01) is parameterized such that the Kohn–Sham eigenvalues are equal to the vertical ionization energies. While this leads to an improvement relative to B3LYP, the transition energies remain too high. SRC2-R2 is the functional that gives transition energies closest to experiment, and this is the only functional for which there is not a large increase for the *K*-edge of the heavier nuclei. This functional was designed for XAS and has a high proportion of HF exchange (91%) in the short range, and this leads to a large change in the core-orbital energies. The R2 parameterization was for elements Na → Ar, but we use these parameters for all elements here.

While the systematic energy shift required by the calculations does not prevent the analysis and interpretation of experimental data,

it remains desirable to have a functional that provides emission spectra that do not require an energy shift to align with experiment. Previous work has found that a high fraction (66%) of HF exchange is required in a standard hybrid functional to provide emission energies close to experimental values.[20] A consequence of this modification of the functional is that the properties of the valence orbitals are adversely affected and the quality of the computed spectra deteriorates. The SRC2-R2 functional used here has 91% HF exchange in the short range. Increasing the percentage of HF to 100% leads to only a small shift to lower emission energies. To reduce the emission

TABLE 2 Variation of the computed energy of the most intense band relative experiment with exchange-correlation functional evaluated using the cc-pCVQZ basis set

Molecule	B3LYP	PBE	CAM-B3LYP	CAM-QTP(01)	SRC1-R2
CH_3OH	+6.4	+7.3	+6.0	+4.7	+4.7
NH_3	+6.8	+7.9	+6.8	+5.7	+4.2
$(CH_3)_2$**C**O	+8.6	+10.6	+8.6	+7.4	+4.7
$(CH_3)_2$**S**O	+8.7	+10.9	+8.7	+7.5	+6.2
C_6H_5**F**	+7.9	+14.0	+7.8	+5.0	+1.3
H_2**S**	+33.7	+44.4	+34.7	+31.9	+7.6
CH_3**Cl**	+38.2	+50.8	+39.2	+36.3	+8.0
CF_3**Cl**	+37.6	+50.9	+38.7	+35.8	+7.5

Bold font denotes the atom that is core-ionized.

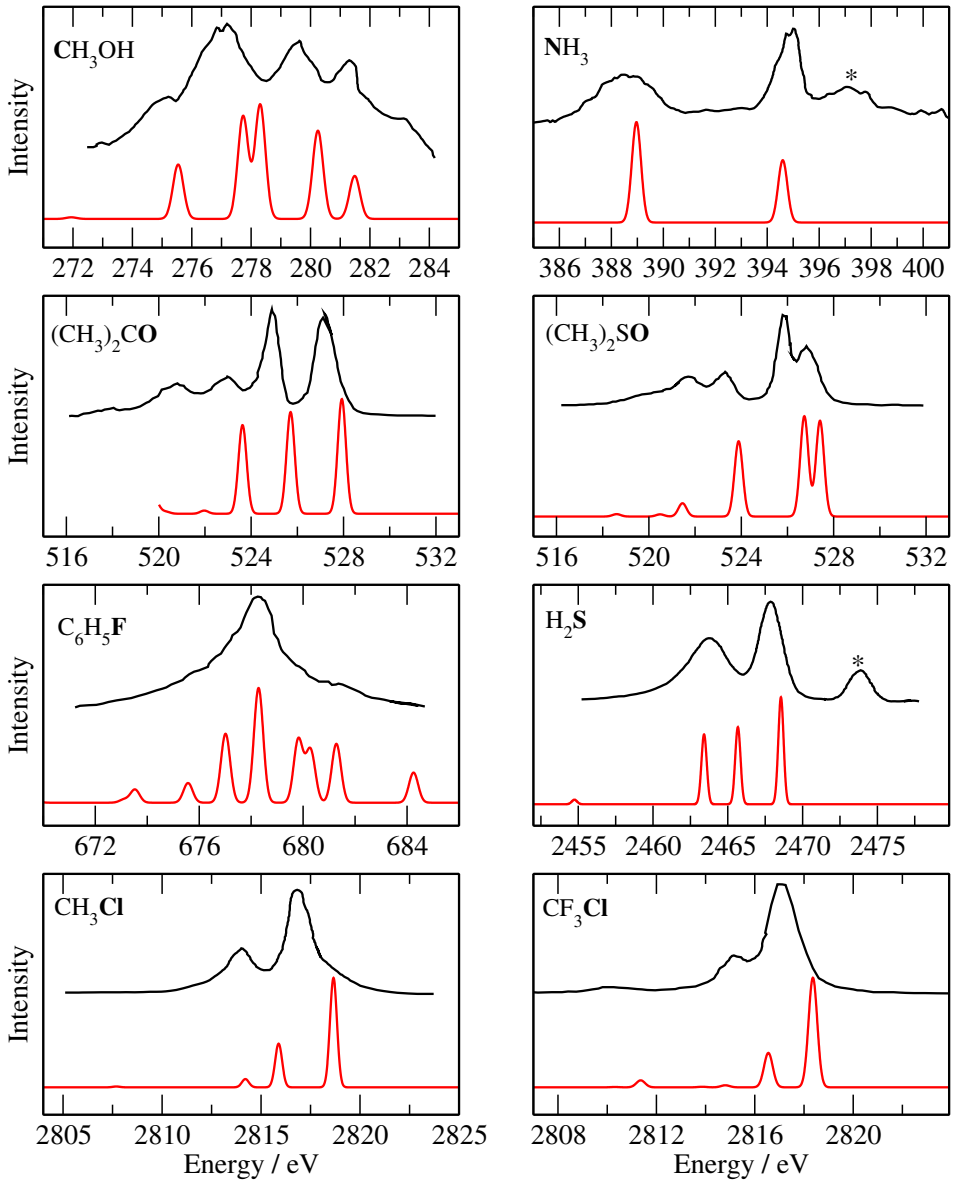

FIGURE 6 Calculated CAM-B3LYP/cc-pCVQZ with energy shift based upon ΔSCF calculation and experimental X-ray emission spectra. Black line: experiment and red line: calculation. * indicates a multi-electron feature. The calculated ΔSCF energy shifts are as follows: CH_3OH: −4.7 eV, NH_3: −7.2 eV, $(CH_3)_2CO$: −7.9 eV, $(CH_3)_2SO$: −7.8 eV, C_6H_5F: −8.6 eV, H_2S: −34.1 eV, CH_3Cl: −37.1 eV and CF_3Cl: −37.2 eV. ΔSCF, Δself-consistent field [Color figure can be viewed at wileyonlinelibrary.com]

energies further requires modification of the short-range attenuation parameter. This leads to a similar problem to the hybrid functionals, that is, the quality of the computed spectra becomes poor. The fundamental difference between the design of functionals for XAS and XES is that for X-ray emission the relevant core orbital is unoccupied. This means that the properties of this orbital are being influenced indirectly through orthogonalisation with respect to the occupied orbital space rather than directly for occupied core orbitals, which is the case for X-ray absorption. This could underlie the need for functional parameters that lead to a poor description of the occupied orbitals.

To generate spectra that requires no information from experiment we adopt a strategy that is often used in the calculation of X-ray absorption spectra, where an energy shift that is applied to the TDDFT computed spectra.[46,47] This shift is determined from a ΔSCF calculation, more specifically, here an extra calculation to determine the ground-state energy of the cation is performed. The energy shift is then determined from the difference between the energy of the highest energy transition in the TDDFT calculation and the corresponding transition energy from a ΔSCF ($E_{\text{core-ionized}} - E_{\text{cation}}$) calculation. The resulting spectra for the CAM-B3LYP/cc-pCVQZ calculations are shown in Figure 6. The position of the spectral bands agrees well with experiment for the molecules considered here. Although further testing would be necessary to determine how well this approach performs for heavier nuclei. There remains an overestimation of the transition energies of about 2 eV for the two chlorine containing molecules. This error may in part be associated with estimation of the relativistic correction which becomes increasingly significant for the chlorine *K*-edge. However, the calculations do show that TDDFT approach does provide a relatively computationally inexpensive method that can be readily applied to give X-ray emission spectra that form a reliable basis to interpret and assign experimental spectra.

4 | CONCLUSIONS

TDDFT provides an efficient approach for the calculation of XES. In this work, the different factors that affect the accuracy of these calculations are explored. Computed spectra evaluated with a large basis set and shifted in energy to align with experiment are in excellent agreement with experiment for the *K*-edge of a range of nuclei. The electronic relaxation of the core orbitals in the intermediate state is an important effect and the neglect of this relaxation leads to spectra that are significantly different from experiment. The calculation of spectra that do not require an additional energy shift to align with experiment is challenging. Investigation of a wide range of available exchange-correlation functionals found the functional predicting emission energies closest to experiment was a short-range corrected functional. However, the calculated emission energies were still systematically too high. Modification of this functional led to a deterioration in the relative energies of the emission bands and worse spectra. Spectra can be calculated by using a ΔSCF calculation of the highest energy transition as a basis to determine the energy shift that needs to be applied. This leads to calculated spectra that provide a reliable description of experiment.

ACKNOWLEDGMENTS

This work was supported by The Leverhulme Trust under Grant [RPG-2016-103].

ORCID

Nicholas A. Besley https://orcid.org/0000-0003-1011-6675

REFERENCES

[1] A. Nilsson, L. Pettersson, *Surf. Sci. Rep.* **2004**, *55*, 49.
[2] L. X. Chen, X. Zhang, M. L. Shelby, *Chem. Sci.* **2014**, *5*, 4136.
[3] M. Chergui, E. Collet, *Chem. Rev.* **2017**, *117*, 11025.
[4] T. Fransson, Y. Harada, N. Kosugi, N. A. Besley, B. Winter, J. J. Rehr, L. G. M. Pettersson, A. Nilsson, *Chem. Rev.* **2016**, *116*, 7551.
[5] N. Lee, T. Petrenko, U. Bergmann, F. Neese, S. DeBeer, *J. Am. Chem. Soc.* **2010**, *132*, 9715.
[6] M. W. D. Hanson-Heine, M. W. George, N. A. Besley, *J. Chem. Phys.* **2017**, *146*, 094106.
[7] H. Agren, J. Nordgren, *Theor. Chim. Acta* **1981**, *58*, 111.
[8] H. Agren, R. Arnberg, J. Muller, R. Manne, *Chem. Phys.* **1984**, *83*, 53.
[9] H. Agren, A. Floresriveros, H. Jensen, *Phys. Scripta* **1989**, *40*, 745.
[10] A. Florersriveros, H. Agren, *Phys. Scripta* **1991**, *44*, 442.
[11] G. Cavigliasso, D. P. Chong, *J. Chem. Phys.* **1999**, *111*, 9485.
[12] D. P. Chong, C. Bureau, *J. Electron Spectrosc. Relat. Phenom.* **2000**, *106*, 1.
[13] Y. Takahata, D. P. Chong, *J. Electron Spectrosc. Relat. Phenom.* **2003**, *133*, 69.
[14] N. A. Besley, A. T. B. Gilbert, P. M. W. Gill, *J. Chem. Phys.* **2009**, *130*, 124308.
[15] I. Tolbatov, D. M. Chipman, *Theor. Chem. Acc.* **2014**, *133*, 1560.
[16] G. Smolentsev, A. V. Soldatov, J. Messinger, K. Merz, T. Weyhermueller, U. Bergmann, Y. Pushkar, J. Yano, V. K. Yachandra, P. Glatzel, *J. Am. Chem. Soc.* **2009**, *131*, 13161.
[17] L. Triguero, L. Pettersson, H. Agren, J. Phys, *Chem. A* **1998**, *102*, 10599.
[18] N. A. Besley, F. A. Asmuruf, *Phys. Chem. Chem. Phys.* **2010**, *12*, 12024.
[19] N. A. Besley, *Chem. Phys. Lett.* **2012**, *542*, 42.
[20] J. D. Wadey, N. A. Besley, *J. Chem. Theory Comput.* **2014**, *10*, 4557.
[21] T. Fransson, A. Dreuw, J. Chem, *Theory Comput.* **2019**, *15*, 546.
[22] Y. Zhang, S. Mukamel, M. Khalil, N. Govind, *J, Chem. Theory Comp.* **2015**, *11*, 5804.
[23] I. P. Roper, N. A. Besley, *J. Chem. Phys.* **2016**, *144*, 114104.
[24] D. R. Mortensen, G. T. Seidler, J. J. Kas, N. Govind, C. P. Schwartz, S. Pemmaraju, D. G. Prendergast, *Phys. Rev. B* **2017**, *96*, 125136.
[25] I. Zhovtobriukh, N. A. Besley, T. Fransson, A. Nilsson, L. G. M. Pettersson, *J. Chem. Phys.* **2018**, *148*, 144507.
[26] A. E. A. Fouda, N. A. Besley, *Theor. Chem. Acc.* **2017**, *137*, 6.
[27] M. A. Ambroise, F. Jensen, J. Chem, *Theory Comput.* **2019**, *15*, 325.
[28] M. W. Hanson-Heine, M. W. George, N. A. Besley, *Chem. Phys. Lett.* **2018**, *699*, 279.
[29] S. Hirata, M. Head-Gordon, *Chem. Phys. Lett.* **1999**, *314*, 291.
[30] A. T. B. Gilbert, N. A. Besley, P. M. W. Gill, J. Phys, *Chem. A* **2008**, *112*, 13164.
[31] V. D. Yumatov, A. V. Okotrub, G. G. Furin, N. F. Salakhutdinov, *Russ. Chem. Bull.* **2004**, *46*, 1389.
[32] J.-E. Rubensson, N. Wassdahl, R. Brammer, J. Nordgren, *J. Electron Spectrosc. Relat. Phenom.* **1988**, *47*, 131.
[33] J. Nordgren, H. Agren, L. O. Werme, C. Nordling, K. Siegbahn, *J. Phys. B At. Mol. Phys.* **1976**, *9*, 295.

[34] R. Mayer, D. W. Lindle, S. H. Southworth, P. L. Cowan, *Phys. Rev. A* **1991**, *43*, 235.
[35] D. W. Lindle, P. L. Cowan, T. Jach, R. E. LaVilla, R. D. Deslattes, R. C. C. Perera, *Phys. Rev. A* **1991**, *43*, 2353.
[36] K. M. Lange, E. F. Aziz, *Chem. Soc. Rev.* **2013**, *42*, 6840.
[37] B. P. Pritchard, D. Altarawy, B. Didier, T. D. Gibson, T. L. Windus, *J. Chem. Inf. Model.* **2019**, *59*, 4814.
[38] Y. Shao, Z. Gan, E. Epifanovsky, A. T. B. Gilbert, M. Wormit, J. Kussmann, A. W. Lange, A. Behn, J. Deng, X. Feng, D. Ghosh, M. Goldey, P. R. Horn, L. D. Jacobson, I. Kaliman, R. Z. Khaliullin, T. Kus, A. Landau, J. Liu, E. I. Proynov, Y. M. Rhee, R. M. Richard, M. A. Rohrdanz, R. P. Steele, E. J. Sundstrom, H. L. Woodcock III, P. M. Zimmerman, D. Zuev, B. Albrecht, E. Alguire, B. Austin, G. J. O. Beran, Y. A. Bernard, E. Berquist, K. Brandhorst, K. B. Bravaya, S. T. Brown, D. Casanova, C.-M. Chang, Y. Chen, S. H. Chien, K. D. Closser, D. L. Crittenden, M. Diedenhofen, R. A. DiStasio Jr., H. Do, A. D. Dutoi, R. G. Edgar, S. Fatehi, L. Fusti-Molnar, A. Ghysels, A. Golubeva-Zadorozhnaya, J. Gomes, M. W. Hanson-Heine, P. H. Harbach, A. W. Hauser, E. G. Hohenstein, Z. C. Holden, T.-C. Jagau, H. Ji, B. Kaduk, K. Khistyaev, J. Kim, J. Kim, R. A. King, P. Klunzinger, D. Kosenkov, T. Kowalczyk, C. M. Krauter, K. U. Lao, A. D. Laurent, K. V. Lawler, S. V. Levchenko, C. Y. Lin, F. Liu, E. Livshits, R. C. Lochan, A. Luenser, P. Manohar, S. F. Manzer, S.-P. Mao, N. Mardirossian, A. V. Marenich, S. A. Maurer, N. J. Mayhall, E. Neuscamman, C. M. Oana, R. Olivares-Amaya, D. P. O'Neill, J. A. Parkhill, T. M. Perrine, R. Peverati, A. Prociuk, D. R. Rehn, E. Rosta, N. J. Russ, S. M. Sharada, S. Sharma, D. W. Small, A. Sodt, T. Stein, D. Stück, Y.-C. Su, A. J. Thom, T. Tsuchimochi, V. Vanovschi, L. Vogt, O. Vydrov, T. Wang, M. A. Watson, J. Wenzel, A. White, C. F. Williams, J. Yang, S. Yeganeh, S. R. Yost, Z.-Q. You, I. Y. Zhang, X. Zhang, Y. Zhao, B. R. Brooks, G. K. Chan, D. M. Chipman, C. J. Cramer, W. A. Goddard III, M. S. Gordon, W. J. Hehre, A. Klamt, H. F. Shaefer III, M. W. Schmidt, C. D. Sherrill, D. G. Truhlar, A. Warshel, X. Xu, A. Aspuru-Guzik, R. Baer, A. T. Bell, N. A. Besley, J.-D. Chai, A. Dreuw, B. D. Dunietz, T. R. Furlani, S. R. Gwaltney, C.-P. Hsu, Y. Jung, J. Kong, D. S. Lambrecht, W. Liang, C. Ochsenfeld, V. A. Rassolov, L. V. Slipchenko, J. E. Subotnik, T. V. Voorhis, J. M. Herbert, A. I. Krylov, P. M. Gill, M. Head-Gordon, *Mol. Phys.* **2015**, *113*, 184.
[39] Y. Imamura, H. Nakai, *Int. J. Quantum Chem.* **2007**, *107*, 23.
[40] A. Mijovilovich, L. G. M. Pettersson, S. Mangold, M. Janousch, J. Susini, M. Salome, F. M. F. de Groot, B. M. Weckhuysen, *J. Phys. Chem. A* **2009**, *113*, 2750.
[41] T. Fransson, I. Zhovtobriukh, S. Coriani, K. T. Wikfeldt, P. Norman, L. G. M. Pettersson, *Phys. Chem. Chem. Phys.* **2016**, *18*, 566.
[42] J. P. Perdew, K. Burke, M. Ernzerhof, *Phys. Rev. Lett.* **1996**, *77*, 3865.
[43] T. Yanai, D. P. Tew, N. C. Handy, *Chem. Phys. Lett.* **2004**, *393*, 51.
[44] Y. Jin, R. J. Bartlett, *J. Chem. Phys.* **2016**, *145*, 034107.
[45] N. A. Besley, M. J. G. Peach, D. J. Tozer, *Phys. Chem. Chem. Phys.* **2009**, *11*, 10350.
[46] P. J. Lestrange, P. D. Nguyen, X. Li, *J. Chem. Theory Comput.* **2015**, *11*, 2994.
[47] A. Chantzis, J. K. Kowalska, D. Maganas, S. DeBeer, F. Neese, *J. Chem. Theory Comput.* **2018**, *14*, 3686.

SUPPORTING INFORMATION

Additional supporting information may be found online in the Supporting Information section at the end of this article.

How to cite this article: Fouda AAE, Besley NA. Improving the predictive quality of time-dependent density functional theory calculations of the X-ray emission spectroscopy of organic molecules. *J Comput Chem*. 2020;1–10. https://doi.org/10.1002/jcc.26153